SIN-CHN SCIENTIFIC PRESS PTE.LTD.

Molecular & Cellular Biomechanics 2025, 22(4), 1251.
https://doi.org/10.62617/mcb1251

Article

Biomechanical influence of organic matter enrichment and sedimentary environment in the Ordos Basin

Siyuan Feng[1,*], Yu Zhang[2], Britney Wu[3]

[1] China University of Petroleum (Beijing), Beijing 102249, China
[2] CNOOC Hainan Branch Company, Haikou 570312, China
[3] Ernst & Young (China) Advisory Limited Beijing Branch, Beijing 100005, China
*** Corresponding author:** Siyuan Feng, F835059870@163.com

CITATION

Feng S, Zhang Y, Wu B. Biomechanical influence of organic matter enrichment and sedimentary environment in the Ordos Basin. Molecular & Cellular Biomechanics. 2025; 22(4): 1251. https://doi.org/10.62617/mcb1251

ARTICLE INFO

Received: 24 December 2024
Accepted: 6 March 2025
Available online: 20 March 2025

Abstract: To study the correlation between organic matter enrichment and sedimentary environment in the Ordos Basin, hydrocarbon source rocks in the region of the eastern edge of the central plain of the basin are selected for analysis. With reference to the related theories of sedimentary rocks and organic geochemistry, the means including pyrolyzed rocks, organic carbon determination, and detection of main trace elements are adopted. The relationship between the regional sedimentary environment and organic matter enrichment is examined after the features of the paleo-sedimentary environment in the study area are examined. At the same time, from the perspective of biomechanics, the concepts of fluid mechanics and material transport are introduced to analyze the influence of hydrodynamic conditions in sedimentary environments on the migration and enrichment of organic matter. The following results were obtained through the study of organic matter enrichment and sedimentary environment in the Ordos Basin: (1) In the analysis of microscopic features, the study area is mainly composed of matrix vitrinite (accounting for more than 68%) and sericite, and also found woody fibers, microbial debris, and pyrite. (2) In organic matter analysis, it was found that the hydrocarbon generation potential (S1 + S2) of the B-S group was divided into multiple levels. According to the relationship, coal can be classified as a good source rock, while the carbonaceous mudstone in the S group belongs to a poor source rock. Group B-T is mainly composed of type III kerogen (humic type). (3) In the analysis of geochemical indicators, the concentrations of Si, Al, and Fe are very high. Further analysis shows that Si and Ti are the main enriched elements, while Re and Mo are abnormally enriched elements. (4) In the analysis of sample physical properties, sample characterization indicates that the source rock is mainly microporous, with few micropores in sandstone, mainly consisting of fractures and medium to large pores. Research has found that there is a correlation between the pore conditions of the sample and organic matter, and the pore volume increases relatively with the increase of organic matter. (5) Organic matter, abdominal muscles, and sediment environment analysis, according to the examination of geochemical indicators, the research area's environment changed significantly from humid to arid and semi-arid conditions at various points during the early, middle, and end of the study period. The salinity of the water body in different regions differed significantly, which was related to the regional climate. The study of the carbon content of organic matter and the characteristics of the sedimentary environment displayed that the redox reaction in the early stages of the region and the local climate had a major influence on the enrichment of organic matter. These two factors became the primary controlling factors affecting the region's organic matter enrichment. The investigation of geological structures and the extraction of local rock gas and minerals can both benefit from the technological assistance this study can offer. At the same time, by introducing the principles of fluid mechanics and material transport in biomechanics, a new perspective is provided for understanding the migration and enrichment mechanism of organic matter in sedimentary environments.

Keywords: organic matter; depositional environments; biomechanics; enrichment; correlation; geochemical indicators

1. Introduction

The Ordos Basin is China's second-largest oil and gas basin and a significant region with abundant mineral resources. With regard to its geological characteristics and resource reserves, the Ordos Basin has emerged as a research hotspot in the fields of mineral exploitation and petroleum exploration in recent years [1]. The Ordos Basin has many unique features in geology as well as tectonics. Its overall outline is a large multi-rotational sedimentary basin with stable sedimentation, argillic migration, and obvious torsion. The basin is surrounded by mountain ranges and the internal topography is relatively low [2]. At the same time, the basin is situated in a large area that spans multiple provinces and regions and is home to abundant natural gas and oil as well as rare metal resources. It is a significant region in China that produces energy resources [3]. The organic matter (OM) enrichment of the basin is closely related to the paleo environment, and this relationship is important for a deeper understanding of the formation of petroleum and other mineral resources [4]. The creation of OM enrichment is a complicated geological process that is impacted by numerous environmental conditions. Related research indicates that one of the main elements influencing the enrichment of OM is the primary productivity level. It is associated with upwelling, river nutrient input, and volcanic activity, and lays the foundation for OM formation in water bodies [5]. In addition, special conditions in the sedimentary environment (SE) will also provide demand for OM formation, such as changes in sedimentary rates in anoxic conditions. In addition, microscopic features such as changes in plant and microbial activities are also closely associated with regional OM enrichment [6]. Biomechanics plays a crucial role in understanding the interaction between organic matter and sedimentary environments. The mechanical properties of sediments influence how organic materials are preserved and transformed over geological time. For instance, the shear strength and compressibility of sediment can affect the burial and compaction processes, ultimately impacting the maturation of organic matter into hydrocarbons. Additionally, the movement and deformation of sediments can facilitate or hinder the migration of fluids, which is essential for the accumulation of hydrocarbons in reservoirs. Thus, integrating biomechanics with geological studies provides a more comprehensive understanding of OM enrichment processes.

From the above research, it can be concluded that the enrichment of organic matter is influenced by various environmental conditions and microbial interactions. Therefore, the next study will be conducted to investigate the OM enrichment in the Ordos Basin in an attempt to better understand the primary controlling factors and their interaction mechanisms of OM enrichment in the basin and to elucidate the relationship between OM enrichment and SE. The objects to conduct the associated investigation are the hydrocarbon source rocks (HSRs) located on the eastern border of the basin's Central Plains.

There are two innovations in the study. One is that the study adopts organic chemistry, geochemistry, and other means to study the SE and OM in the study area

to ensure the accuracy of the study. The second is to establish a correlation model between SE and OM enrichment, which will further provide a basis for the study of regional OM enrichment. The research material will speed up the advancement of geological exploration technology in China and offer crucial technical references for the geological analysis and development of mineral, oil, and gas resources.

2. Methods

2.1. Regional information

The Ordos Basin is the second largest sedimentary basin in China, with a total area of about 370,000 square kilometers [7]. Beginning in the north with the Mount Yinshan and Daqing Mountains, the Ordos Basin extends southward to the Qinling Mountains, westward to the Helan and Liupan Mountains, and eastward to the Luliang and Taihang Mountains [8]. The basin features a mild slope drop, is a large-scale multi-rotation craton basin, rises in the east and falls in the west, and is high in the east and low in the west. The climate of the basin is temperate continental, with 2700–3200 h of annual sunshine and an average annual temperature of 5.3 ℃–8.7 ℃ [9].

The Shixi block on the eastern margin of the Central Plains of the basin is selected for the study and analyzed. The area is located in Liulin County, Shanxi Province, and contains the Shanxi Formation (Group S), Benxi Formation (Group B), Taiyuan Formation (Group T), and Lower Stone Box Formation (Group X). The block strikes in a north-south position and dips towards the west. Analyzing the geological structure of the block, there are five faults developed in the area, including two normal faults and three reverse faults. In addition, the stratigraphic characteristics of the study area remain continuous and complete. The stratigraphy in the area shows an old to new distribution, including the interface of paleo, meso, and neo stages. Further research, the Paleozoic stratigraphy of the study block includes the Permo-Triassic, Carboniferous, and Cenozoic [10]. In addition, the Benxi-Shanxi Formation of the Carboniferous is presented as a coal mine layer, in which the rock types include chert, mudstone, etc., and the thickness ranges from 31 m to 49 m. The thickness of the Shanxi Formation in the block ranges from 99 m to 140 m, and the rock types are mainly powder sandstone and mudstone.

2.2. Experimental methods

2.2.1. Sample collection

A total of 12 samples from 17 boreholes in the experimental area were selected as samples for analysis as follows. Group S had 3 samples, including coal, carbonaceous mudstone, and sandstone, which are one sample each. Group B had 3 samples, including coal, carbonaceous mudstone, sandstone, and one sample. Group T had 2 samples containing coal, carbonaceous mudstone, and sandstone, all in one piece. Group X sample had 4 pieces, sandstone totaling 4 pieces. The details are shown in **Table 1**.

The 12 collected samples were cleaned of impurities by ultrasonic waves and deionized water. Then the samples were air-dried at 60 ℃ for 10 h using an

air-drying oven. At the end of the drying process, the samples were crushed and milled, screened with 80 mesh, and stored in an airtight dry environment.

Table 1. Sample collection information.

Stratigraphic unit	Depth (m)	Rock type	Sample number	Sedimentary facies
Group X	1340	Mudstone	Ap-1	Fluvial facies
	1410	Silty mudstone	Ap-3	
	1440	Sandy mudstone	Ap-7	
	1490	Middle sandstone	Ap-13	
Group S	1555	Mudstone	Ap-13	Delta facies
	1610	Siltstone	Ap-15	
	1655	Coal	Ap-20	
Group T	1600	Pelitic siltstone	Ap-30	Carbonate platform facies
	1710	Coal	Ap-31	
Group B	1712	Sandstone	Ap-32	
	1730	Coal	Ap-33	
	1750	Black mudstone	Ap-34	

2.2.2. Pyrolysis of rocks

The pyrolysis of rocks was mainly carried out by the multi EA 5000 pyrolysis analyzer. Before the experiment, the sample was weighed at 100 mg in a crucible, and the heating rate and initial temperature were set, and the temperature was raised to 1100 ℃. Then the samples were cracked under oxygen-free nitrogen gas. The hydrocarbons in the cracked samples were detected by a Schembechler EXPEC 3100, and the carbon and oxygen gas produced by the cracking were detected by a FLIR G346 infrared device.

2.2.3. Organic carbon testing

Organic carbon detection was mainly carried out through the model CS4600 equipment for organic carbon content (TOC) detection. Specific process: the porcelain crucible was calcined at a high temperature of 1050 ℃ for 2 h, and the ground sample was placed in the crucible. HCL (1 mol/L) was added to remove the inorganic carbon in the sample. Then the treated samples were put into the porcelain crucible and placed in the drying box at 80 ℃ for 30 min. Finally, the carbon dioxide and sulfur dioxide absorbance were detected by using CS460 equipment, and the final TOC was obtained by comparing the elements with the total mass.

2.2.4. Element detection

The detection of the elements in the samples was mainly accomplished by ICP-MS. Specific process: 1 g of the sample was put into the porcelain crucible and heated in the ma-boiling furnace (1000 ℃) for 1 h, and then waited for the sample to cool down for the loss on ignition detection. Sulfur content: 0.25 g NaOH was put into a 0.05 g sample reagent and dissolved in an Ag crucible at 800 ℃. Next, HCl was added to it in the specification of 5 mL. Finally, the solution was adjusted to 260 ml, and elemental detection was carried out by ICP-MS.

2.2.5. Rock characterization

The rock characterization was mainly done at Chengdu University of Technology, including the preparation of pulverized coal light film and the detection of microscopic components. Among them, the crushed coal sample wormwood was mixed into the crucible with a ratio of 2:1. It was heated to 95 ℃, during which the mixture was stirred continuously. When the sample material was completely melted, the mixture was inlaid into the machine, and the pressure was set to 3.4 MPa for 40 s. Then, the mill was used to grind with water. Finally, the preparation of pulverized coal photoflakes was completed by polishing with 0.05 μm polishing cloth treatment.

Analysis of rock pore specification: The rock samples were cut in columns, keeping the length at 5 cm, and distillation was used to remove impurities and ensure that the crevices were clean. Then, the samples were put into the vacuum pressurization equipment for 1 h of vacuuming. Finally, the samples were dried of water, and the pore specifications of the samples were obtained by nuclear magnetic resonance experiments. In addition, the sample volume was calculated using the drainage method.

2.2.6. Carbon isotope analysis of casein root

The rock samples were processed by acid-foam heavy liquid extraction, and the extraction of casein root was realized by heavy liquid extraction [11]. Carbon isotope analysis was carried out by mass spectrometer with casein root as the test sample. In this, the humidity of the detection environment was kept at 50% RH and the temperature was kept at 25 ℃.

2.3. Assessment of indicators

Indicators for OM enrichment assessment: Hydrocarbon potential (S1 + S2) indicates the hydrocarbon potential. The TOC reflects the percentage of organic carbon. Hydrogen index (HI) reflects OM hydrogen content [12].

OM maturity assessment index: Reflectance of specular plasma (Ro) is used to reflect OM maturity. The higher the index, the higher the maturity. The maximum peak pyrolysis temperature (Tmax) indicates the temperature at which the OM pyrolysis process produces the maximum amount of hydrocarbons. Casein element ratios are O/C as well as H/C [13,14].

Geographical indicators: The upper crust mean (UCC) reflects the abundance of elements in a region or sample. The enrichment factor *tr* (ratio of oxide content to UCC) is used to determine the degree of enrichment of metal elements. Among them, $5 < tr$ (abnormal enrichment), $1.1 < tr \leq 5$ (enrichment type), $0.9 \leq tr \leq 1.1$ (similarity type), $tr < 0.9$ (loss type). The characteristics of climate change are reflected by the Sr/Cu = *Yr* ratio, where $Yr > 10$ (dry), $5 \leq Yr \leq 10$ (semi-dry and semi-humid), and $Yr < 5$ (humid) [15].

The sedimentary climate environment is reflected by comparing the Sr/Cu and Rb/Sr correlation maps, as well as the SiO_2 and $Al_2O_3 + K_2O + Na_2O$ correlation maps. The important indicator of paleo environmental sedimentation reflected by paleosalinity is represented by Sr/Ba = IO. Among them, IO > 1, 0.5 < IO < 1, and IO < 0.5, respectively refer to saline, brackish, and freshwater environments. The parent rock's weathering is represented by the chemical corrosion index (CIA),

which has values between 50 and 100. The larger the value, the more severe the corrosion. The value of the ancient climate index (*C* value) is arid at (0, 0.2), semi-arid at (0.2, 0.4), semi-humid and semi-arid at (0.6, 0.8), and humid at (0.8, 1). The ancient productivity is represented by NiEF and CuEF, and the enrichment of elements is reflected by the Ni and Cu content [16].

Physical characteristics: Pores smaller than 2 nm are considered micropores, pores between 2 nm and 50 nm are considered mesopores, and pores larger than 50 nm are considered macropores. Other indicators: Characteristics of ancient environmental oxidation-reduction indicators are δU, Ni/Co, and V/(V + Ni) [17].

3. Result

3.1. Microanalytical characterization

Figure 1 shows the characterization of the HSR sample. From the microscope, matrix specular plastids and filamentous plastids can be found. Further analysis of the samples can find woody fibers in the samples, such as crumbly lazy plasmodesmata. In addition, microbial remains, such as fungi, are found in some matrix specular bodies, and pyrite is detected in some samples. Overall, the samples contain a relatively high percentage of specular plasmodesmata, amounting to more than 68%. The inert plasmas are above 10% and the rest are mineral components.

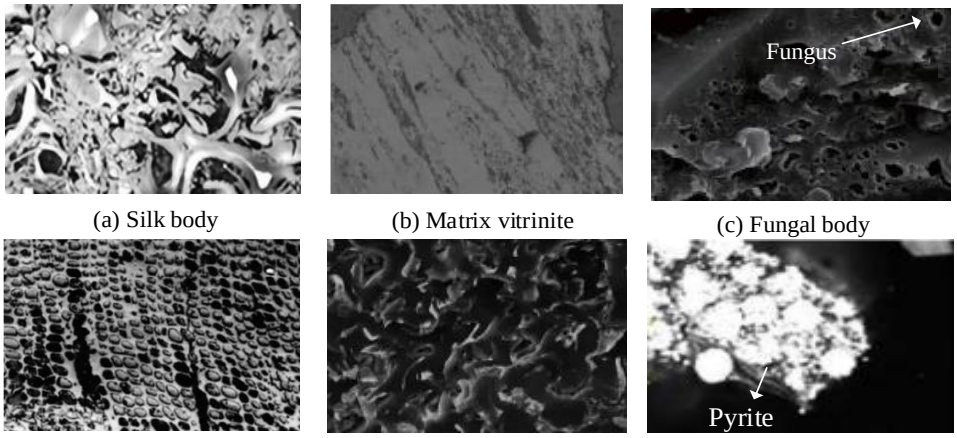

(a) Silk body (b) Matrix vitrinite (c) Fungal body

(d) Detrital inertinite (e) Structural vitrinite (f) Pyrite

Figure 1. Reflection microscope image of source rock.

3.2. Organic matter characterization

Figure 2a displays the findings of the analysis of the HSR scenario of experimental Group B-S and the correlation between the TOC value and S1 + S2. Among them, the hydrocarbon potential (S1 + S2) is divided into several classes. According to the relationship coal, it can be categorized as a better HSR, and carbonaceous mudstone within the Group S belongs to a worse HSR. The study divides I, II1, II2, and III according to the HSRs in the study, which correspond to the three types of sapropel, humus-sapropel, sapropel-humus and humus, respectively. Using the casein carbon isotope expressed as δ13C, the OM types at different depths are displayed in **Figure 2b**. The outcomes display that Groups B-T are mainly dominated by type III casein (humus type), and the characteristics of this

type of OM are mainly dominated by gas production. Meanwhile, Group B is mainly dominated by type II2 casein, with oil as well as gas production occurring in some areas. Continuing to analyze the carbon isotopes of casein, the carbon isotopes are lighter in the sedimentary stage of Group B, while their carbon isotope values are significantly heavier in the sedimentary stage of Group T. The carbon isotopes become lighter as they continue to the Group S, and the factors that lead to this situation may be related to the SE of the region and the factors of OM formation. For example, Group B is mainly composed of OM in the form of algae, while terrestrial plants are involved in the formation of OM in Group T, and aquatic plants are mainly dominant in Group S.

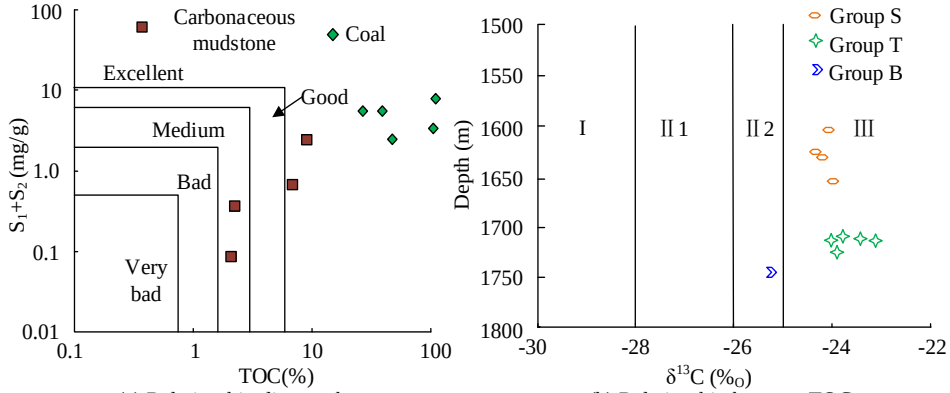

(a) Relationship diagram between TOC and S_1+S_2 in source rocks

(b) Relationship between TOC and $\delta^{13}C$ in source rocks

Figure 2. Analysis of organic matter characteristics in Groups B-S.

Next, the RO indicator as well as Tmax are used to analyze the OM maturity. **Table 2** displays the values of the indicators for the various phases of maturity.

Table 2. Classification of organic matter maturity.

Thermal evolution stage of source rocks	**immature**		**mature**		**Highly mature**	**overmature**
Ro (%)	< 0.50–0.60	0.50–0.70 (0.80)	0.70 (0.80)–1.00	1.00–1.35	1.35–2.00	> 2.00
Oil and gas maturity stage	Immature, biogas	Low maturity oil	Peak of oil generation	Light oil	Gas condensate—wet gas	Dry gas
Tmax (℃)	< 430	430–440	440–450	450–460	460–500	> 500

In **Table 2**, the higher the Ro value, the more obvious the OM maturity. The same is true for the Tmax indicator, where the higher the value, the more pronounced the OM maturity. The maturity of different groups of samples is compared, as shown in **Table 3**. The outcomes illustrate that all the collected OM samples are over-mature, and the Tmax values of all the samples are close to each other, which are all above 500 °C.

Table 3. Maturity status of samples in different groups.

Sample number	Lithology	Stratum	Ro/%	Tmax/℃
AP-13-1	Charcoal mudstone	Group S	2.13	556
AP-20-1	Coal	Group S	2.12	571
AP--13-2	Charcoal mudstone	Group S	2.13	572
AP-20-2	Coal	Group S	2.15	561
AP-31-1	Coal	Group T	2.18	571
AP-31-2	Coal	Group T	2.19	570
AP-31-3	Coal	Group T	2.24	571
AP-30	Pelitic siltstone	Group T	2.25	570
AP-33	Coal	Group B	2.26	571

3.3. Analysis of geochemical indicators

Figure 3 shows the UCC content test results of samples from Group B-X. According to the results, the content of Ni and Cu in the source rock is significantly higher than that in sandstone. The average enrichment coefficient of the source rock is 1.70, while the average enrichment coefficient of sandstone is 5.85, and the Fe, Al, and Si contents in the samples are all higher. The EF of Si and Ti in sandstone is greater than 1 (mean 5.85), which may be due to the input of terrestrial debris (such as quartz and titanium minerals) or stable sedimentary environments. The low EF of the source rock (1.70) reflects the enrichment of organic matter accompanied by the adsorption of clay minerals, which inhibits the enrichment of detrital elements. Continuing the analysis, the main enriched elements in the sample are Si and Ti. From **Figure 3a**, it can be seen that the enrichment coefficients of Si and Ti in sandstone samples are both greater than 1, indicating relative enrichment. Other elements show a basic depletion in sandstone, while elements such as Co, Ni, Cr, etc. also show depletion in coal and carbonaceous mudstone, which may be influenced by the type of parent rock, sedimentary environment and redox conditions, as well as differentiation during weathering processes. In addition, the analysis found that the abnormally enriched elements were mainly Re and Mo, and the Re anomaly may be related to the acidity and environment of the rock mass. The EF of Si and Ti in sandstone is greater than 1 (mean 5.85), which may be due to the input of terrestrial debris (such as quartz and titanium minerals) or stable sedimentary environments. The low EF of the source rock (1.70) reflects the enrichment of organic matter accompanied by the adsorption of clay minerals, which inhibits the enrichment of detrital elements. The enriched elements are Hf, Pb, Sb, Cd, Zr, Nb, In, Bi, and similar enrichment mainly includes Ta, Ga, Zn, Be, and Cu.

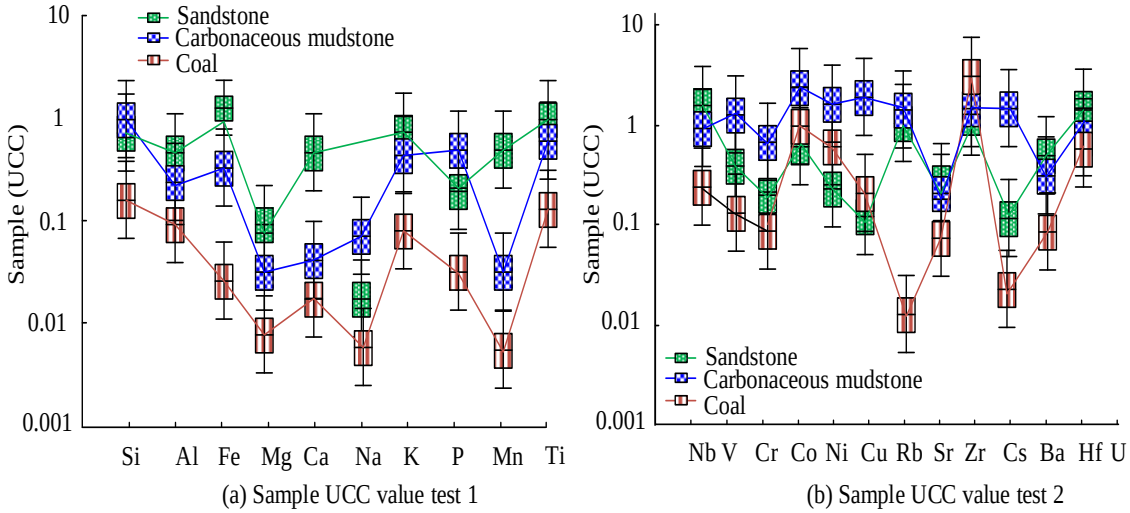

Figure 3. UCC content of samples from Group B-X in the study area.

Next, the elemental conditions in the regional paleo environment are studied. The Rb/Sry and Sr/Cu relationships used in **Figure 4a** reflect the paleo environment during the sedimentary period. Among them, the Group S is mainly semi-humid during the sedimentation period, while the Group S, T group, and Group B are mainly warm and humid during the sedimentation period. Subsequently, Al_2O_3 + K_2O + Na_2O and SiO_2 are used to backwash the SE, and the detection results are consistent with Sr/Cu detection. This suggests that warm, humid, or semi-humid climates are the primary characteristics of the ancient environment during the sedimentary period. In addition, from **Figure 4b**, it can be analyzed that the weathering level of the sedimentary period samples is mainly above average.

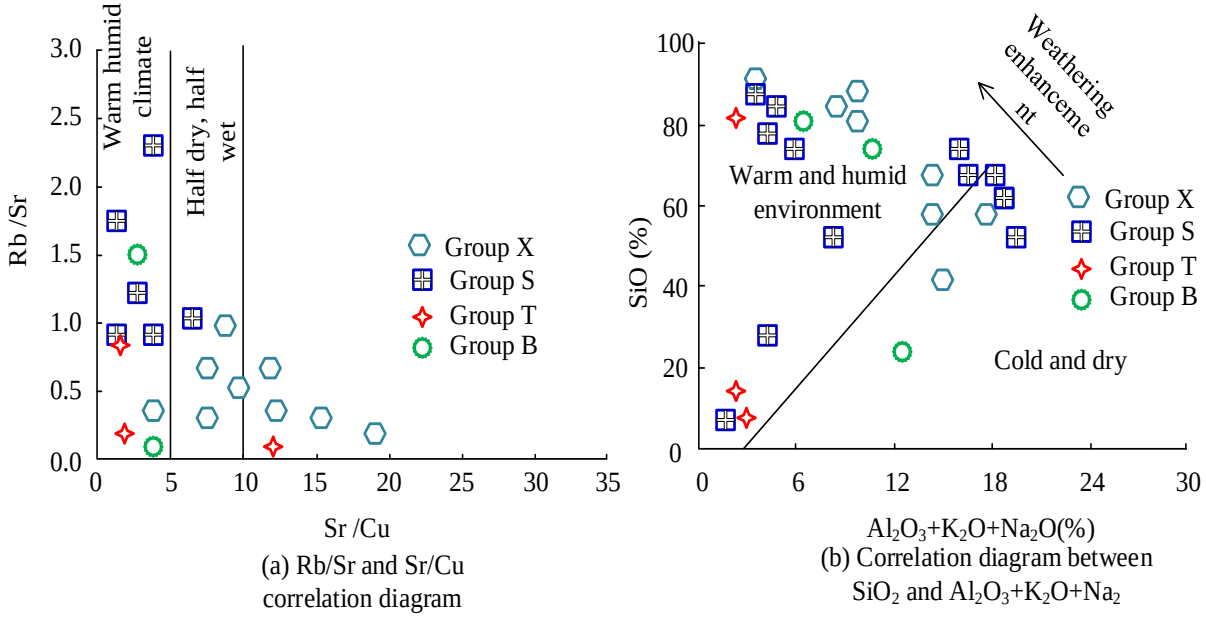

Figure 4. Analysis of paleo environmental climate change in Groups B-X.

Figure 5 displays the outcomes of the salinity analysis of the paleo environment. The results show that the salinity value of Group X is between 0.16

and 0.56, and most of them are less than 0.5, which is in a freshwater environment. The salinity value of Group T ranges from 0.51 to 1.61, which is in a semi-saline water environment. Group B has salinity values ranging from 0.46 to 2.71 and generally shows a freshwater environment. Group S has salinity values in the range of 0.51 to 0.15 and an overall freshwater environment.

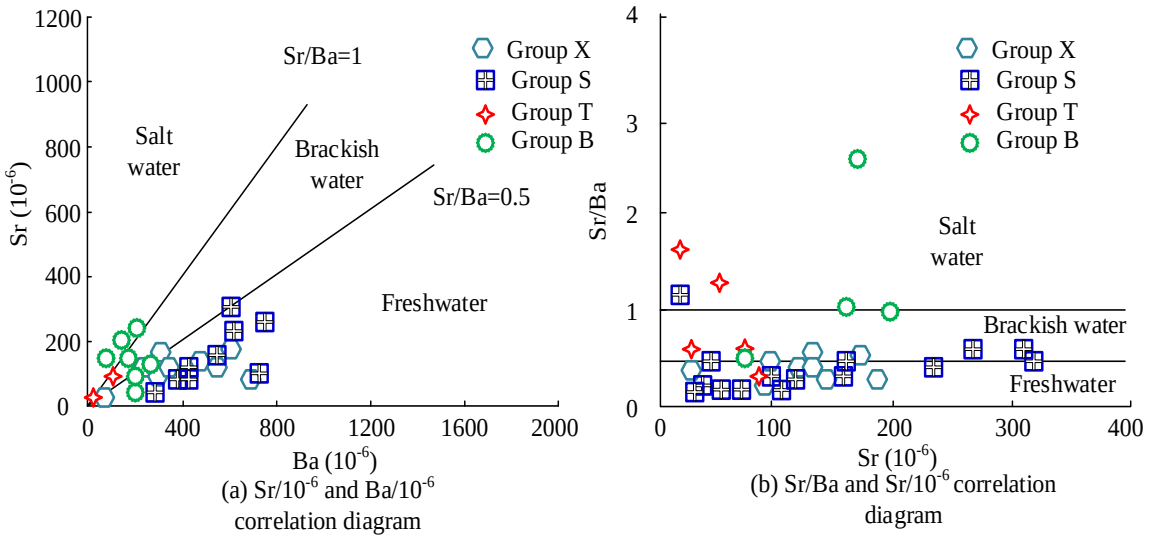

Figure 5. Analysis of paleo environmental salinity in Groups B-X.

3.4. Physical characterization of rock samples

Figure 6 shows the results of the pore size (PS) distribution of the samples detected using NMR. Among them, the Group X sandstone is mainly mesopores, accounting for 2.045%, followed by 1.524% macropores. The S-group sandstone is mainly 1.725% macroporous and 2.524% mesoporous, with only 0.015% microporous. The coal and carbonaceous mudstone in Group S has 0.154% micropores compared to 2.624% mesopores and 0.741% macropores. In the sandstone of Group T with Group B, the predominantly mesoporous is about 3.25%. In addition, there are 0.895% macropores. The percentage of mesopores as well as macropores in Group B is 2.255% and 0.542%, respectively. In general, micropores are less developed in sandstone and more developed in coal and carbonaceous mudstone in general.

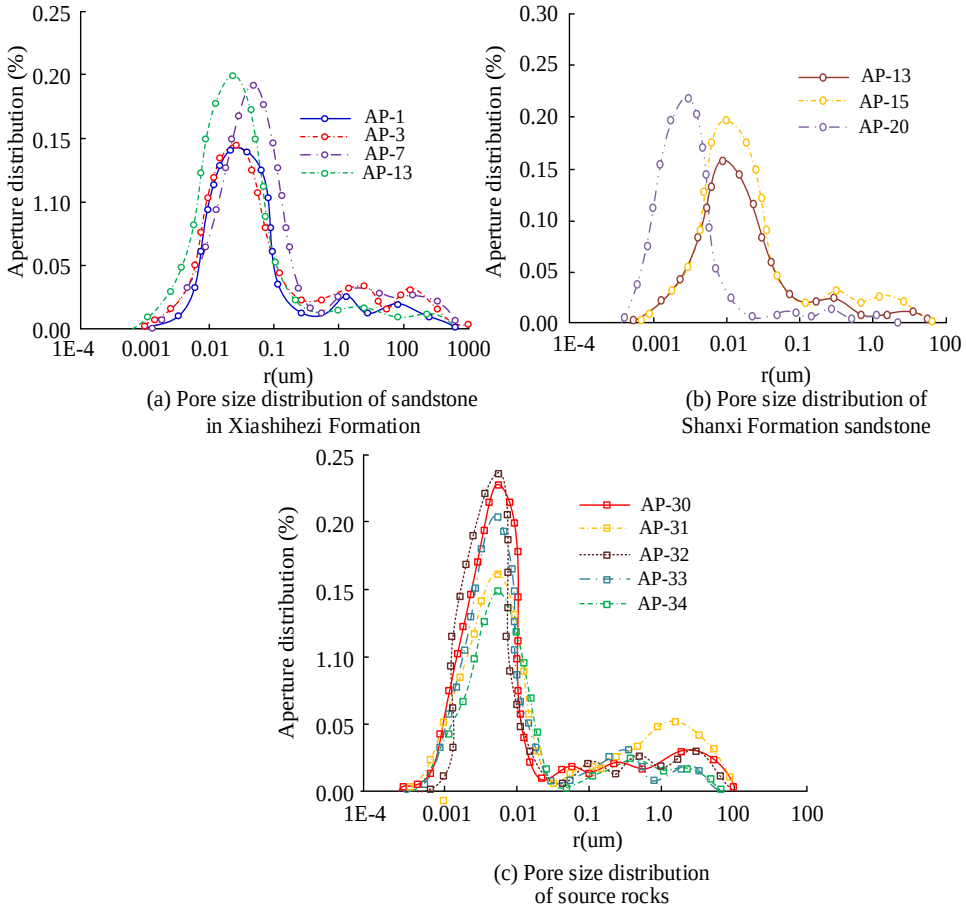

Figure 6. Sample pore size distribution.

Figure 7 shows the relationship between pore size and TOC. In the Ordos Basin, there is a close relationship between pore characteristics and organic matter enrichment. Research has shown that in carbonaceous mudstone, the volume of mesopores and micropores is positively correlated with total organic carbon (TOC), indicating that the larger the pores, the higher the organic matter content. In coal, the micropore volume, total volume, and macropore volume are negatively correlated with TOC, indicating that as the pores increase, the organic matter content actually decreases. In addition, the development process of intermediate pore volume in coal first increases and then decreases. Usually, an increase in organic matter content will lead to an increase in pore size, but after reaching saturation, the pore volume will decrease. This indicates that pore size and volume have a significant impact on the migration and accumulation of organic matter. In the process of organic matter enrichment, smaller pore sizes are beneficial for the adsorption and preservation of organic matter, while larger pore sizes may promote the migration and diffusion of organic matter. Therefore, pore characteristics play a crucial role in the enrichment of organic matter and the generation of oil and gas.

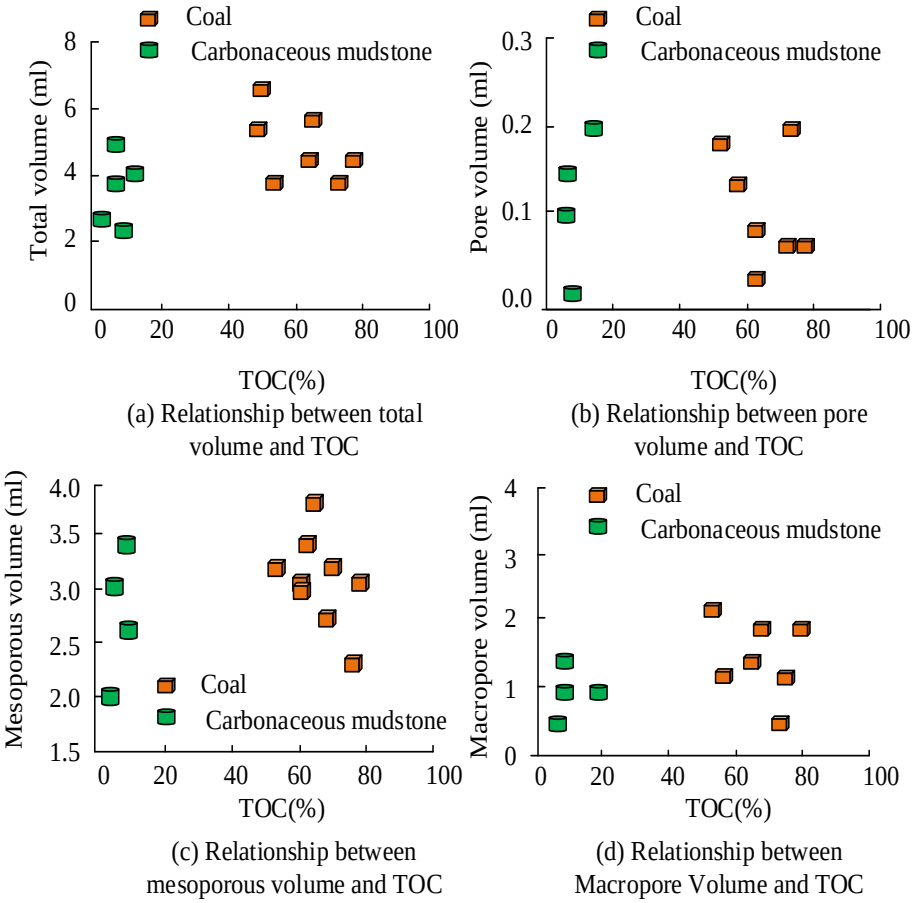

(a) Relationship between total volume and TOC

(b) Relationship between pore volume and TOC

(c) Relationship between mesoporous volume and TOC

(d) Relationship between Macropore Volume and TOC

Figure 7. Relationship between aperture and TOC.

3.5. Correlation analysis between organic matter enrichment and paleo environmental

Figure 8 shows the analysis of the effect of paleo environmental redox on regional OM enrichment. The water environment favors OM enrichment when oxygen content is lacking, and its markers include Ni/Co, V/Cr, etc. Among them, only δU has a good correlation with TOC, with an R^2 of 0.6436, and other key indicators are not correlated. This result suggests that coal as well as carbonaceous mudstone mainly showed strong reducing properties in the formed water body during the paleo environmental period.

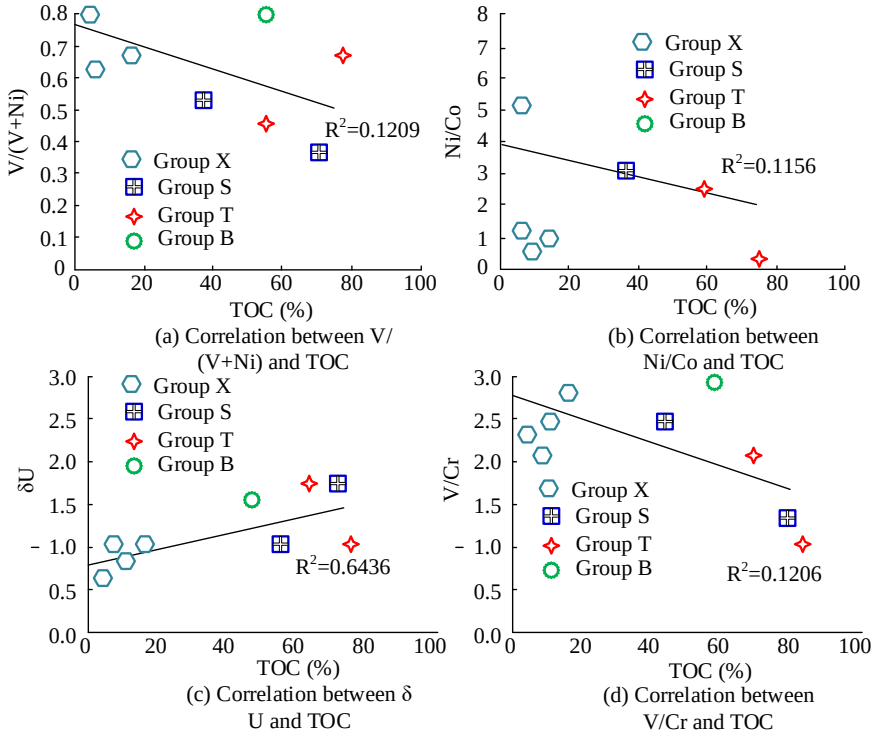

Figure 8. Analysis of the relationship between paleo environmental oxidation-reduction and regional organic matter enrichment in Group B-S.

Figure 9 shows the analysis of the relationship between ancient environmental oxidation-reduction and regional organic matter enrichment. The Sr/Cu ratio can effectively distinguish and distinguish environmental climate, but it is susceptible to interference from redox conditions in sedimentary environments. The Rb/Sr ratio reflects the intensity of weathering, as Sr is more easily leached and lost in humid climates, but may be biased by the mineral composition of the parent rock (such as volcanic material). In addition, the CIA index quantifies the degree of chemical weathering through the ratio of Al_2O_3 to migratory elements, directly related to precipitation conditions, but sensitive to the composition of the original rock. It is necessary to comprehensively analyze the environmental climate and weathering conditions to ensure their rationality. From the results, it can be seen that environmental indicators such as humid environments and weathering intensity are correlated with TOC. Especially in humid environments, it is beneficial for biological reproduction, which is conducive to the growth and reproduction of organisms and provides abundant organic matter sources for the development of source rocks. According to the results, TOC and CIA have the best correlation, with an R^2 of 0.0778, while Sr/Cu reflects climate and humidity changes, and Rb/Sr reflects sedimentary characteristics. According to the results, there is a significant negative correlation between TOC and Rb/Sr, indicating that paleoclimatic conditions do not have a significant controlling effect on the enrichment of organic matter in the study area. However, TOC is negatively correlated with the organic content of middling coal in Group T, which may be caused by the intervention of other conditional factors. In addition, the higher the weathering degree of CIA, the greater the input of terrestrial sources during the OM sedimentary stage, and it has a

positive impact on the formation of organic matter. In addition, based on the above research, it can be found that sediments with high shear strength can effectively resist hydrodynamic disturbances (such as bottom flow erosion or biological disturbances), reduce organic matter resuspension and oxidative decomposition. Compressibility affects preservation efficiency by regulating the pore structure of sediments: The high permeability of low compressibility sediments (such as sandy sediments) accelerates oxygen diffusion and promotes organic matter oxidation; the low porosity of high compressibility fine-grained sediments (such as clay) can maintain a hypoxic environment and inhibit microbial degradation. All of these are beneficial for the burial and preservation of organic matter.

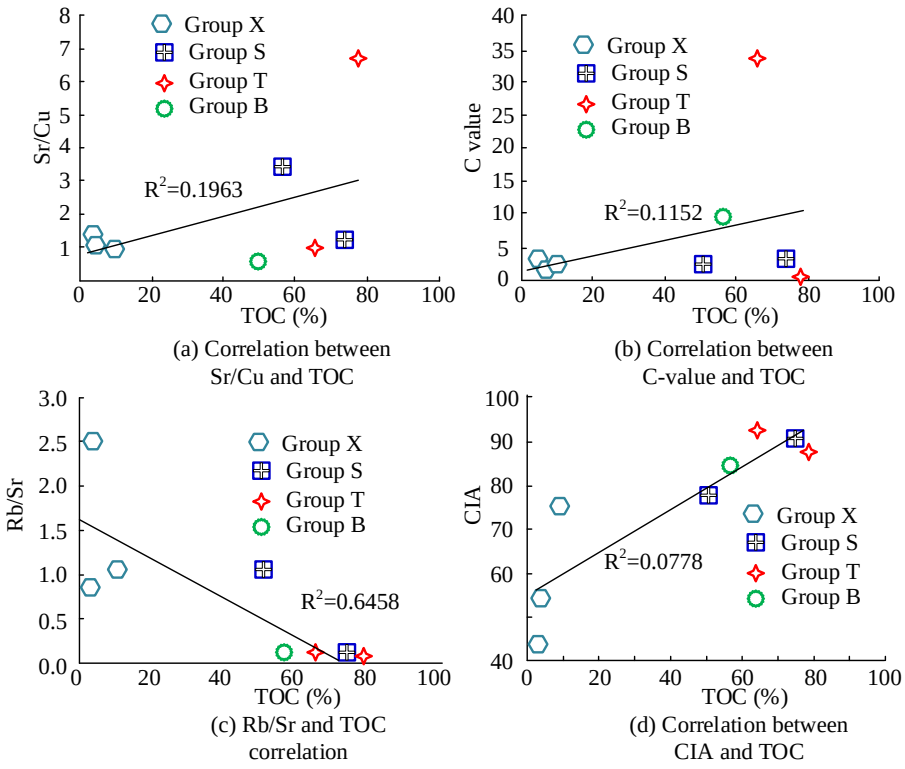

Figure 9. Correlation between paleo environmental climate and organic matter enrichment in Groups B-S.

Figure 10 shows the effect of paleo environmental salinity on OM enrichment. There is a correlation effect between the salinity of the sedimentary water body and TOC, which is mainly reflected in its positive effect on both OM preservation and biological development. In contrast, in the paleo productivity analysis, CuEF is not correlated with OM, while it is less correlated with NiEF. This indicates that the productivity in the paleo environmental period does not bring an effective control effect on OM enrichment. In addition, the migration and enrichment of organic matter in the Ordos Basin are significantly influenced by biomechanical mechanisms, mainly manifested in the regulation of organic matter preservation efficiency by controlling hydrodynamic conditions and sediment organic matter interactions through paleo environmental salinity. Moderate salinity (brackish to brackish water) enhances water stratification and anaerobic environments, inhibits microbial degradation and oxidation, and thereby improves the organic matter

retention rate. Meanwhile, an increase in salinity may promote the flocculation of clay minerals and organic matter, accelerating the settling and burial of organic matter particles. It is worth noting that the correlation between ancient productivity indicators (CuEF, NiEF) and TOC is weak, suggesting that organic matter enrichment mainly depends on preservation conditions rather than initial productivity. This biomechanical process is reflected in the stability of sedimentary environments driven by salinity, which forms a physical chemical coupling mechanism conducive to the long-term storage of organic matter by limiting the input of terrestrial debris (reducing dilution effects) and enhancing chemical flocculation.

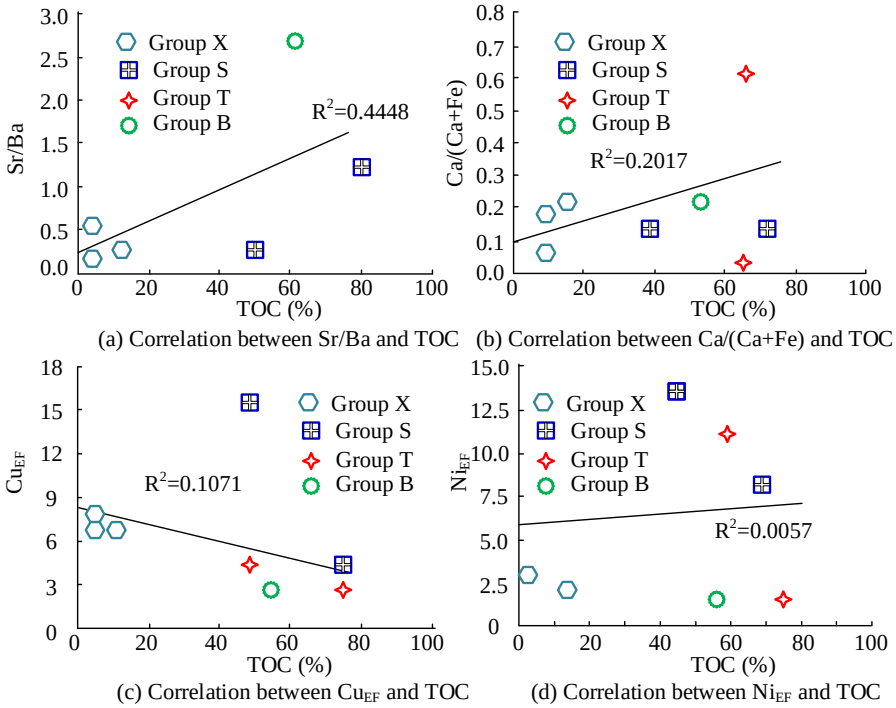

Figure 10. Correlation between paleo environmental salinity, productivity, and organic matter enrichment in Groups B-S.

4. Discussion

The study of OM enrichment is of great significance for oil and coal mining. In order to effectively analyze the main controlling factors of OM enrichment in the Ordos Basin, research is conducted on the sedimentary environment of the study area by combining geochemistry, paleo environmental climate, rock physical properties, and other factors. Analysis of research results: (1) Microscopic feature analysis: The hydrocarbon source rock samples are mainly composed of vitrinite (accounting for more than 68%), followed by inertinite (more than 10%), containing a small amount of pyrite and microbial debris, indicating that the OM source is mainly terrestrial higher plants, with local algal contributions. The high content of vitrinite reflects a sedimentary environment dominated by weak oxidation and weak reduction, while inertinite indicates partial input of igneous debris, which is consistent with the volcanic activity background around the Ordos Basin [18]. (2) OM characteristic analysis: The kerogen in the study area is mainly of type III (humic type) (B group, T

group), with locally developed type II2 (humus humic mixed type) in group S. The δ 13C values indicate a transition of OM sources from algae (B group) to terrestrial plants (T group). The Ro value (2.12%~2.26%) and Tmax (556~571 ℃) indicate that the samples are in the over-mature stage, mainly producing gas, which is related to the long-term tectonic subsidence and thermal evolution history of the basin. (3) Analysis of geochemical indicators: Element enrichment shows enrichment of Si and Ti (with an average EF of 5.85 in sandstone), and abnormal enrichment of Re and Mo in source rocks (EF > 5), reflecting the superposition of terrestrial debris input and volcanic hydrothermal activity. The Sr/Ba ratio (0.16~2.71) indicates the transition of paleosalinity from freshwater (X group) to brackish water (T group), while the Sr/Cu ratio (mean 3.8) and CIA index (65~78) indicate that the climate during the sedimentary period was mainly semi-humid to semi-arid, with moderate chemical weathering. (4) Analysis of physical properties of rock samples: Source rocks are mainly microporous (< 2 nm) (accounting for 0.15%~0.74%), while sandstone is dominated by mesopores (2–50 nm) and macropores (>50 nm). There is a non-linear relationship between TOC and pore volume: the pore volume in mudstone is positively correlated with TOC (R^2 = 0.64), while the micropore volume in coal decreases with increasing TOC, which may be related to OM compaction and mineral filling. (5) Correlation analysis between OM enrichment and sedimentary environment: OM enrichment is controlled by paleoclimate, salinity, and redox conditions. Wet climate (Sr/Cu < 5) and brackish water environment (Sr/Ba > 0.5) promote algal blooms (initial productivity increase), while low terrestrial inputs (CIA > 65) and reduced bottom water (V/(V + Ni) > 0.6) inhibit OM degradation. There is a significant positive correlation between δU and TOC (R^2 = 0.64), indicating that a hypoxic environment is the key to preservation, which is consistent with the “preservation theory” of the Chang-7 Formation in Ordos. Volcanic activity (tuff interlayers) triggers a “delayed” burst of productivity through nutrient inputs (such as P, Fe), driving abnormally high TOC values (> 30%).

From the above research, it can be seen that the OM enrichment mechanism in the Ordos Basin exhibits a dual control feature of “productivity preservation”. The coupling effect between the paleoclimate (semi-humid, semi-arid) and paleosalinity (freshwater, brackish water) in the study area provides a basis for the flourishing of algae, which is consistent with the “volcano hydrothermal productivity” model proposed by Liu et al. [19]. The generally high Ro value (> 2.1%) reflects the strong influence of the Yanshanian tectonic thermal event on the southeastern edge of the basin, leading to over maturation of OM, which is consistent with the research conclusions of Jiang Longyan et al. on the thermal evolution of the Chang-7 Member in Fuxian area. The pore structure of hydrocarbon source rocks, dominated by micropores (accounting for > 60%), indicates that the adsorption capacity of OM is constrained by pore size, which is consistent with the experimental conclusion of Liu et al. on the pore size TOC relationship of terrestrial shale [20]. In addition, the abnormal enrichment of Re and Mo suggests the contribution of deep hydrothermal activity to element migration, which needs to be further verified in conjunction with Cd isotopes. The research results support the view that “preservation conditions dominate”, but the instantaneous enhancement effect of volcanic activity on productivity still needs to be considered in high TOC intervals (such as the Chang 73

subsection). This mechanism provides new ideas for predicting the “sweet spot” of terrestrial shale oil [21,22].

5. Conclusion

The study of OM enrichment is of great significance to oil and coal mining. To effectively analyze the main controlling factors of OM enrichment in the Ordos Basin, the study combined geochemistry, paleo environmental climate, and physical characteristics of rocks to investigate the SE of the study area. The results of experimental analysis showed that microbial remains and plant debris were detected in the rock samples, and the coal was a high-quality HSR. The elemental tests of the samples revealed high contents of Si, Al and Fe, and Re and Mo were anomalously enriched elements. Among them, the Re anomaly might be related to the acidity in the rock body and the environment. In the paleo environmental and climatic analyses, the study area was mainly characterized by a humid-warm climate, and the water environment was mainly dominated by semi-saline and brackish water. In the pore analysis of the samples, the coal rock samples were more microporous, while the sandstone was mainly dominated by mesopores as well as macropores. Moreover, it was further found that the pore volume decreased with the gradual saturation of OM content. Finally, the relationship between organic carbon and SE was analyzed. It was found that the OM enrichment was related to the paleo environmental climate, water environment characteristics, and redox conditions, such as temperature, humid environment, and paleo-salinity level, all of which are favorable to the formation of organic carbon TOC. Through the above studies, it was realized that the formation of OM in the Ordos Basin was influenced by many factors. Among them, the regional paleo environmental climate conditions and chemical effects are the key to influencing the regional OM enrichment. However, the study also has shortcomings, and the research samples are limited. To give oil and gas exploration and resource development a more precise scientific foundation, more OM-enriched locations must be investigated, and more influencing elements must be examined.

Supplementary materials: Experimental equipment: Carbon and sulfur analyzer (CS4600, Steel Research Nanogram); Rock pyrolysis analysis instrument (Multi EA 5000, Jena, Germany); MAT 252 Mass Spectrometer (ELEMENTRAC CS-i, ELTRA); Inductively Coupled Plasma Mass Spectrometer (Agilent 720, Jena PlasmaQuant MS); Drying box (TRX-24, Chuanyu Instrument); Hydrogen flame ionization detector (EXPEC 3100, Shenbei Scientific Instrument); Infrared detector (FLIR G346, FLIR Systems, Inc); Vacuum pressurization equipment (ZYB-III, Jiangsu Lianyou Scientific Instrument); Refractive light microscope (CFI Plan Apo, Nikon, Japan). Experimental reagent: Hydrochloric acid (1 mol/L, Wuxi Tengsheng Chemical); Dichloromethane (purity ≥ 99%, Shanghai Aladdin Biochemical Technology); Methanol (purity ≥ 99.9%, developed by Shanghai Runjie Technology); Petroleum ether (purity 120, Shandong Yukang Chemical); Hydrofluoric acid (40% concentration, Honeywell International Inc, USA); Sodium hydroxide (analytical grade, Bolinda Technology); Hydrochloric acid (analytical

grade, Merck KGaA, Germany).

Author contributions: Conceptualization, SF and YZ; methodology, SF; software, BW; validation, SF, YZ and BW; formal analysis, BW; investigation, YZ; resources, SF; data curation, YZ; writing—original draft preparation, SF; writing—review and editing, SF; visualization, BW; supervision, YZ; project administration, SF; funding acquisition, SF. All authors have read and agreed to the published version of the manuscript.

Ethical approval: Not applicable.

Conflict of interest: The authors declare no conflict of interest.

References

1. Shi J, He D. Tectonic characteristics and evolution of the middle segment of the Jinxi flexure fold belt in the eastern margin of the Ordos Basin. Chinese Journal of Geology. 2024; 59(3): 723-731. doi: 10.12017/dzkx.2024.051
2. Zhong S, Tan X, Wei L, et al. Tectono-sedimentary evolution and oil-gas geological significance of first to third member of Ordovician Majiagou Formation in Ordos Basin, NW China. Petroleum Exploration and Development. 2024; 51(5): 1202-1216.
3. He Y, Xue T, Li Z, et al. Development technologies for Triassic Chang 7 shale oil in Ordos Basin: A case study of Qingcheng Oilfield, NW China. Petroleum Exploration and Development. 2023; 50(6): 1245-1258. doi: 10.11698/PED.20230248
4. Liao J, Xiao W, Long L, et al. Sedimentary characteristics, formation conditions, and distribution mechanisms of beach bar sand bodies of Chang 82 submember, southwest Ordos Basin. Energy Science & Engineering. 2024; 12(5): 1835-1854. doi: 10.1002/ese3.1692
5. Mei Q, Guo R, Zhou X, et al. Pore structure characteristics and impact factors of laminated shale oil reservoir in Chang 73 sub-member of Ordos Basin, China. Journal of Natural Gas Geoscience. 2023; 8(4): 227-243. doi: 10.1016/j.jnggs.2023.07.003
6. Lyu Q, Fu J, Luo S, et al. Sedimentary characteristics and model of gravity flow channel-lobe complex in a depression lake basin: A case study of Chang 7 Member of Triassic Yanchang Formation in southwestern Ordos Basin, NW China. Petroleum Exploration and Development. 2022; 49(6): 1323-1338. doi: 10.1016/s1876-3804(23)60352-0
7. Niu X, Fan L, Yan X, et al. Enrichment conditions and resource potential of coal-rock gas in Ordos Basin, NW China. Petroleum Exploration and Development. 2024; 51(5): 972-985. doi: 10.11698/PED.20230656
8. Yu S, Zhao Z, Zhu Y, et al. Reservoir Characteristics and Formation Model of the Bauxite Gas Reservoir: The Benxi Formation in the LX Block, Northeast of Ordos Basin, China. ACS Omega. 2024; 9(16): 18127-18136. doi: 10.1021/acsomega.3c10097
9. Li YF, Zhang CL, Liang F, et al. New material of Coniopteris simplex from the Middle Jurassic of the Ordos Basin, Inner Mongolia, China and implications on its spatio-temporal distribution and paleogeography. Journal of Palaeogeography. 2024; 13(2): 199-211. doi: 10.1016/j.jop.2024.03.001
10. Cao Y, Jin Z, Zhu R, et al. The influence of extraction of various solvents on chemical properties on Chang 7 shale, Ordos Basin, China. Solid Earth. 2023; 14(11): 1169-1179. doi: 10.5194/se-14-1169-2023
11. Chen R, Wang F, Li Z, et al. Detrital zircon geochronology of the Permian Lower Shihezi Formation, northern Ordos Basin, China: time constraints for closing of the Palaeo-Asian Ocean. Geological Magazine. 2022; 159(9): 1601-1620. doi: 10.1017/s0016756822000498
12. Liu X, Liu Y, Lu Z, et al. Study on the characteristics and influencing factors of Chang 7 ultralow-porosity and low-permeability reservoirs in the Heshui area, Ordos Basin. Interpretation. 2022; 10(4): T581-T593. doi: 10.1190/int-2021-0138.1
13. Hu G, Shao Y, Liu X, et al. Paleoseismic evolution of the central section of the Serteng Shan fault at the northern Ordos Block (North China) since the Late Pleistocene. International Geology Review. 2023; 65(20): 3272-3285. doi: 10.1080/00206814.2023.2180778
14. Wen L, Huang W, Zhang Y, et al. Mineralogy and Geochemistry of Rare Earth Elements in Carboniferous-Permian Coals at

the Eastern Margin of the Ordos Basin. ACS omega. 2024; 9(30): 32481-32501. doi: 10.1021/acsomega.4c00546

15. Akhtar AA, Cruger Ahm AS, Higgins JA. Geochemical fingerprints of early diagenesis in shallow-water marine carbonates: Insights from paired δ44/40Ca and δ26Mg values. Geochimica et Cosmochimica Acta. 2024; 383: 57-69. doi: 10.1016/j.gca.2024.08.002
16. Chen D, Zhu Y, Wang W, et al. Pore structure of tight sandstones with differing permeability: The He 8 Member of the Middle Permian Lower Shihezi Formation, Gaoqiao area, Ordos Basin. Energy Science & Engineering. 2023; 12(1): 117-135. doi: 10.1002/ese3.1621
17. Gingras MK, MacEachern JA, Dashtgard SE, et al. The Teichichnus Ichnofacies: Its neoichnological basis and identification in the rock record. Sedimentology. 2024; 72(2): 408-441. doi: 10.1111/sed.13246
18. Martínez M, Brearley AJ. Calcium phosphates associated with chondrules in the CR chondrite Queen Alexandra Range (QUE) 99177: Evidence for solar nebular and parent body processes. Geochimica et Cosmochimica Acta. 2025; 391: 127-143. doi: 10.1016/j.gca.2024.12.020
19. Xu T, Jia A, Huang Y, et al. Distribution and Main Controlling Factors of Gas and Water in Tight Sandstone Gas Fields: A Case Study of Sudong 41-33 Block in Sulige Gas Field, Ordos Basin, China. ACS Omega. 2024; 9(19): 20807-20818. doi: 10.1021/acsomega.3c09154
20. Chen K, Qü X, Xie Q, et al. High-Inclination Coring of Chang-63 of the Yanchang Formation in Huaqing Oilfield, Ordos Basin: Implications for Ancient Flow Direction and Fracture Orientation. Engineering. 2023; 15(01): 24-46. doi: 10.4236/eng.2023.151003
21. Matheson EJ, Malone JD, Pufahl PK, et al. Late Ordovician ironstone and its relation to ocean redox instability, climate and glaciation. Sedimentology. 2024; 72(2): 631-665. doi: 10.1111/sed.13247
22. Klöcking M, Wyborn L, Lehnert KA, et al. Community recommendations for geochemical data, services and analytical capabilities in the 21st century. Geochimica et Cosmochimica Acta. 2023; 351: 192-205. doi: 10.1016/j.gca.2023.04.024